ACS APPLIED MATERIALS & INTERFACES

Letter

www.acsami.org

Resolving the Chemical Nature of Nanodesigned Silica Surface Obtained via a Bottom-up Approach

Hakim Rahma,[†,‡] Thierry Buffeteau,[†,‡] Colette Belin,[†,‡] Gwenaëlle Le Bourdon,[†,‡] Marie Degueil,[†,‡] Bernard Bennetau,[†,‡] Luc Vellutini,[†,‡,*] and Karine Heuzé*[,†,‡]

[†]Université de Bordeaux, ISM UMR 5255, F-33400 Talence, France

[‡]CNRS, ISM UMR 5255, F-33400 Talence, France

Supporting Information

ABSTRACT: The covalent grafting on silica surfaces of a functional dendritic organosilane coupling agent inserted, in a long alkyl chain monolayer, is described. In this paper, we show that depending on experimental parameters, particularly the solvent, it is possible to obtain a nanodesigned surface via a bottom-up approach. Thus, we succeed in the formation of both homogeneous dense monolayer and a heterogeneous dense monolayer, the latter being characterized by a nanosized volcano-type pattern (4−6 nm of height, 100 nm of width, and around 3 volcanos/μm^2) randomly distributed over the surface. The dendritic attribute of the grafted silylated coupling agent affords enough anchoring sites to immobilize covalently functional gold nanoparticles (GNPs), coated with amino PEG polymer to resolve the chemical nature of the surfaces and especially the volcano type nanopattern structures of the heterogeneous monolayer. Thus, the versatile surface chemistry developed herein is particularly challenging as the nanodesign is straightforward achieved in a bottom-up approach without any specific lithography device.

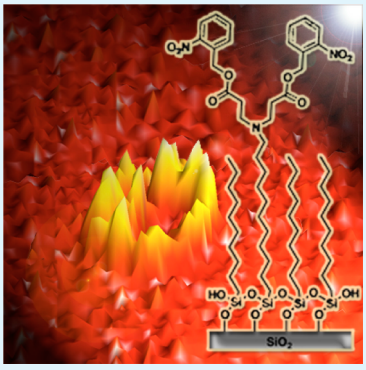

KEYWORDS: *monolayer, nanodesign, surface analysis, atomic-force microscopy, IR spectroscopy*

Controlling surface properties and biological interfaces at the nanometer scale have become essential challenges in biotechnology. In this field, many applications such as biosensing,[1,2] biological studies (culture or interactions),[3,4] drug/gene delivery carriers,[5] or implantable medical devices[6,7] are surface-demanding. The key element for molecular recognition and specific interactions studies is to control biomolecules distribution with nanopatterns from small proteins to cells via chemically modified substrates. Surface modifications by nanopatterning techniques[8−11] to generate chemically or topography resolved patterns, generally lithographies techniques, require highly specialized devices such as lasers for ablation, scanning probe,[12,13] or e-beam,[14] which are often expensive and used for a limited number of biological studies. So, investigations in new strategies of surface modifications are critical for the development of controlled, easily scaled-up, and repeatable modified nanopatterned surfaces.[15]

Silica surfaces are often good candidates for chemical surface modification with the formation of resistant and dense packed organosilanes self-assembled monolayers.[1,9,12,16−18] Besides the strong demand for more and more sophisticated and highly specific functional organosilanes, functional dendritic organosilanes represent a great interest because of their singular architecture and tunable functionalities fitting with many applications.[19−23] As well, dendritic molecules established themselves their structures as leadership in many fields of biotechnology.[24,25] Their highly controlled structures together with their large number of peripheral functions, make them one of the most well-defined chemical tool.[26−28]

Most authors[29−32] studied the deposition of dendrons or dendrimers on bare surfaces (HOPG, mica, or gold) and they reported molecular arrangements in a molecular scale patterning or nano and submicropatterned surfaces (dots or rings arrangements). Other authors reported the grafting of dendritic thiols[33−38] molecules or inserted into alkane-thiol SAMs on gold substrates for biotechnology. Some of them highlighted phase segregation between the different thiols molecules grafted on the surface reflected by the formation of nanometer scale molecular domains. Also, Fréchet and co-workers[39] reported the covalent grafting of functional triethoxysilane dendrimer on TiO_2 designing a dendrimer monolayer dense enough for its use for scanning probe lithography. More recently, Archer and co-workers[40] reported a step-growth grafting of carbosilane dendrons on silicon wafers for a deep study of surface's physical properties. Finally, Wöhrle and co-workers[41] reported the covalent grafting of PAMAM dendrimer on amino-silylated glass substrate leading to the formation of a polymeric functional thin film for nucleic acid and protein microarrays. Although, some thin films or monolayers made up of covalent grafted dendrons/dendrimers on bare or amino-silylated SiO_2 substrates are reported in the

Received: May 30, 2013
Accepted: July 15, 2013
Published: July 15, 2013

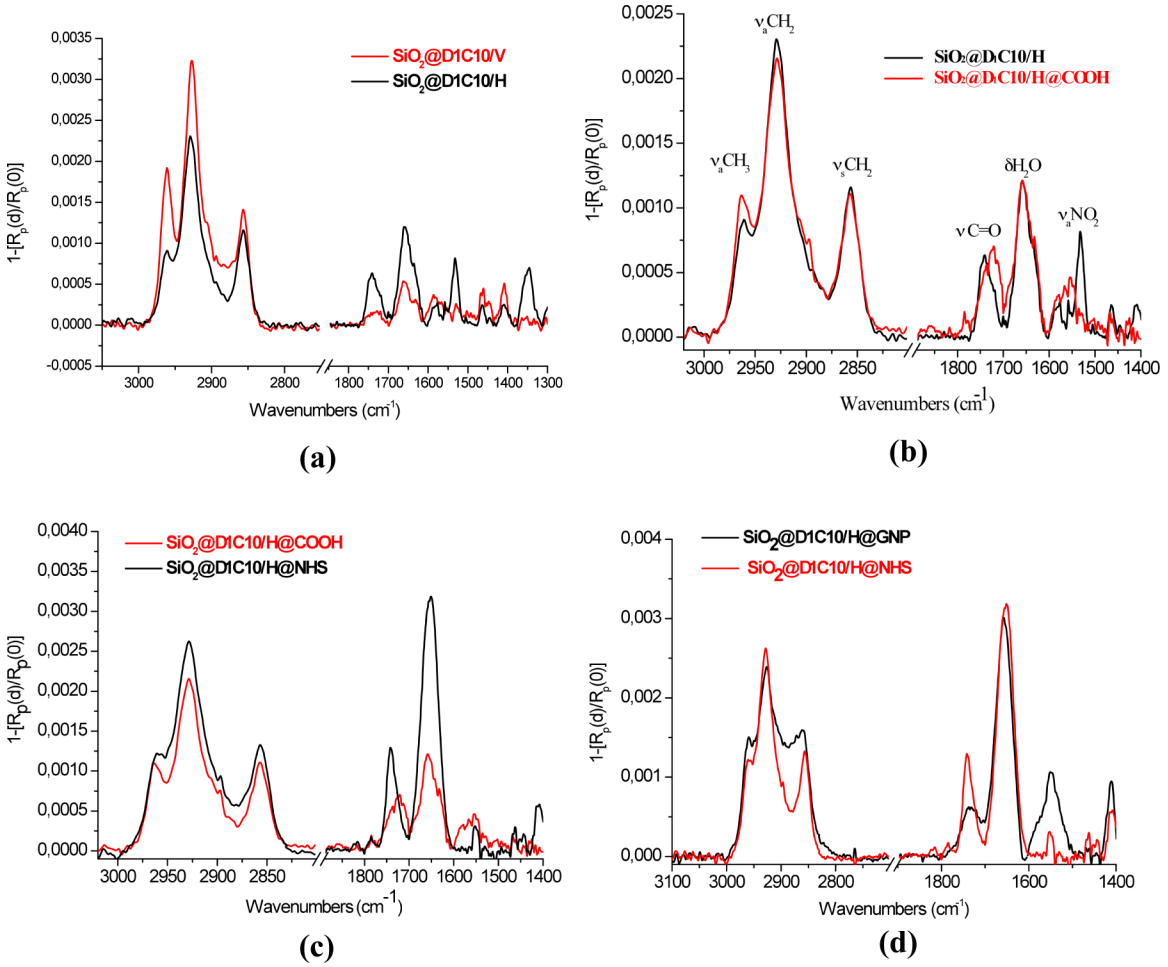

Figure 1. (a) PM-IRRAS spectra of **SiO_2@D1C10/H** and **SiO_2@D1C10/V**. (b) PM-IRRAS spectra of **SiO_2@D1C10/H** before and after photodeprotection, (c) before and after activation of COOH groups, and (d) before and after immobilization of GNPs.

literature, but none of them emphasized a controlled nanodesign of the surface via a bottom-up approach.

In this paper, we report on a straightforward method for the design of functional nanodomains of silica substrate with an organic layer constituted of dendritic functional coupling agents following a bottom-up approach. We describe the synthesis of a new dendritic functional coupling agent of first generation possessing two protected carboxylic acid groups and a trichlorosilane anchoring site. We show that the covalent grafting of this coupling agent together with decyltrichlorosilane on silica substrates can be optimized leading to two different modified surfaces (an homogeneous and a nanodomains designed surface). The nanodomains patterned surface shows comparable spatial control possibly obtained by conventional costly lithography techniques. The chemical nature of the nanodomain designed surface was analyzed through specific functionalization with gold nanoparticles coated with PEG-NH_2 polymer in order to settle the chemical nature of nanodomains of the surface.

Dendrons are often used to modify chemically inorganic or organic surfaces as they show specific geometries, sizes and easily tunable functionalities. The optimization of their grafting allows controlling properties of the surface as wetting, roughness, hardness and reactivity of corresponding materials. In this present work, we build on the dendritic structure of the organosilane coupling agent to increase the functionalization[42] of the surface and to afford enough anchoring sites for the covalent immobilization of target materials. The grafting of dendrons on solid supports and more specifically on SiO_2 substrates can be achieved by either divergent or convergent approaches. (i) The divergent route consists in the building of the dendritic structure from the bare substrate in a solid state chemistry way, and (ii) the convergent route consists in the synthesis of the dendron in solution following by the grafting (silanization) of the dendron on the substrate in the final step. The latter strategy, that we have selected, allows a better control of organic molecular structures,[43] in contrast with the divergent strategy, which often generates structural defects on surfaces.[44]

Synthesis of Dendritic Coupling Agent D1. Dendritic coupling agent **D1** was synthesized as described in (see Scheme S1 in the Supporting Information). Acrylate derivative **1** was prepared from acryloyl chloride and 2-nitrobenzyl alcohol in the presence of triethylamine in dry dichloromethane, and was isolated after purification over silica gel chromatography (90% yield). Then, acrylate **D1** was obtained by double Michael addition[45] of amine group of 11-amino-1-undecene[46] with 2-nitrobenzyl acrylate compound **1** in DMF.[47] Reaction medium was stirred for 3 days at 50 °C, and the compound **D1** was obtained in quantitative yield after purification over silica gel chromatography. Coupling agent **D1** was obtained in a few

dx.doi.org/10.1021/am402071t | ACS Appl. Mater. Interfaces 2013, 5, 6843−6849

grams scale and stored shielded from light, at room temperature, for several months.

Silanization of Silica Substrate with a Mixture of Hydrosilylated D1/Decyltrichlorosilane Coupling Agents (25/75). Dense functional layers can be obtained on silica surfaces by the silanization of functional alkyltrichlorosilanes coupling agents in optimized conditions.[48] In this work, we aimed to obtain well-defined and dense functional surfaces so we investigated the silanization of silica substrate with a mixture of two organosilanes: the hydrosilylated dendron **D1** and decyltrichlorosilane. Indeed, dendritic structure of **D1** strongly affects the packing of the organosilanes at the surface and prevents from obtaining a densely packed monolayer except in the case of a dilution with a coassembled linear organosilane. Dilution of functional coupling agents with nonfunctional coupling agents is a strategy often used[49−51] and permits generally to enhance some properties of the surface as a space control of immobilized biological species.[52] Also, it was demonstrated that the formation of SAMs by the self-assembly of a mixture of two silanes is an efficient strategy to form chemical functional patterns on gold or silica surfaces.[53] In this context, optimization of the experimental conditions of the silanization step was performed while it plays a decisive part in the surface functions distribution (patterning with a phase segregation between the two coupling agents), as it was reported by some authors in the case of a gold surface.[54] The grafting of a mixture of hydrosilylated **D1** coupling agent with decyltrichlorosilane (25/75) was performed as shown in (Scheme S2 in Supporting Information). The ratio between dendritic coupling agent and linear coupling agent was chosen in order to minimize steric hindrance and to favor self-assembly of molecules during the formation of the monolayer. The grafting process was studied by varying the nature of the solvent and we demonstrated that two different surfaces **SiO_2@D1C10/H** and **SiO_2@D1C10/V** can be obtained depending on the solvent used, respectively, $CHCl_3/C_6H_{12}$ (25/75) and toluene. The temperature of the silanization reaction was fixed at 5 °C to prevent the formation of aggregates by hydrolysis condensation reaction in solution. In both cases, optimal reaction time was found to be 45 min by measuring the evolution of contact angle, PM-IRRAS spectra, and AFM images (rms parameter) of the surfaces.

First, an homogeneous monolayer **SiO_2@D1C10/H** was fully characterized by PM-IRRAS spectroscopy, AFM, and contact angle measurements. The hydrophobic nature of the surface was characterized by a contact angle value of 80° ± 2. Comparing with the contact angle measured on the bare SiO_2 surface (0°), this value confirms the chemical modification of the surface. PM-IRRAS spectrum of **SiO_2@D1C10/H** is presented in (Figure 1a). We observed, in the 3100−2700 cm^{-1} spectral range, bands characteristic to the methyl and the methylene stretching vibrations and, in the 1800−1300 cm^{-1} region, some bands characteristic to the carbonyl and nitro stretching vibrations. The methylene antisymmetric and symmetric stretching vibrations are observed at 2928 cm^{-1} ($\nu_a(CH_2)$) and at 2856 cm^{-1} ($\nu_s(CH_2)$), respectively, suggesting that the alkyl chains are quite disordered in the grafted molecules and contain significant gauche defects. The characteristic vibration of the terminal methyl group of decyltrichlorosilane corresponding to the antisymmetric stretching vibration $\nu_a(CH_3)$ is observed at 2961 cm^{-1}. The observed bands at 1740, 1531, and 1345 cm^{-1} are attributed, respectively, to the $\nu C{=}O$, $\nu_a NO_2$ and $\nu_s NO_2$ vibrations associated with the dendritic structure of the organosilane coupling agent. The presence of these bands confirms that the two organosilanes are grafted on the surface. Note that the presence of the band around 1640 cm^{-1} can be associated with water molecules adsorbed at the monolayer surface.

Analysis of AFM height images (5 μm × 5 μm) showed an homogeneous appearance of the surface and the presence of only a few polysiloxanes aggregates (Figure 2a). The phase image of AFM is consistent with a unique chemical nature on the whole surface (Figure 2b). Moreover, the roughness rms = 0.4 nm (calculated on the whole height image) is very close to the bare surface roughness obtained before the grafting (0.2 nm).

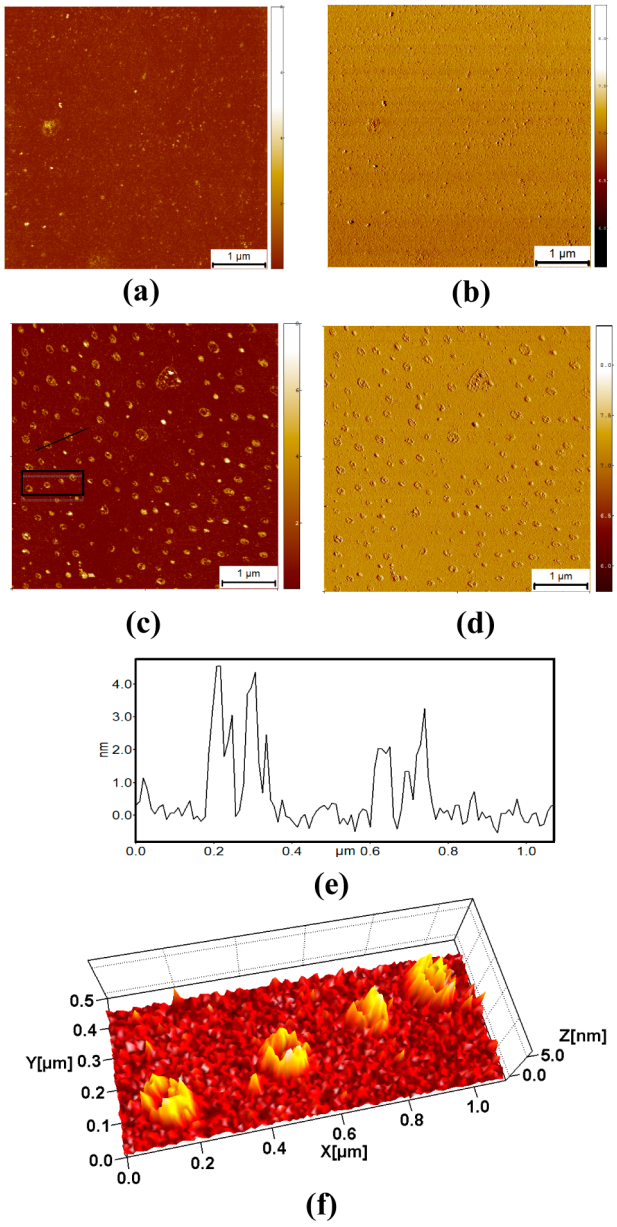

Figure 2. AFM images (5 μm × 5 μm) of grafted **SiO_2@D1C10/H** surface: (a) Height image, (b) phase image. AFM images (5 μm × 5 μm) of grafted **SiO_2@D1C10/V** surface: (c) Height image, (d) phase image. (e) Topography along a line drawn in c. (f) 3D representation of the nanovolcano structure of c.

dx.doi.org/10.1021/am402071t | ACS Appl. Mater. Interfaces 2013, 5, 6843−6849

Scheme 1. Chemical Modification and Covalent Immobilization of GNPs on the Functional Silica Surfaces SiO_2@D1C10/H and SiO_2@D1C10/V

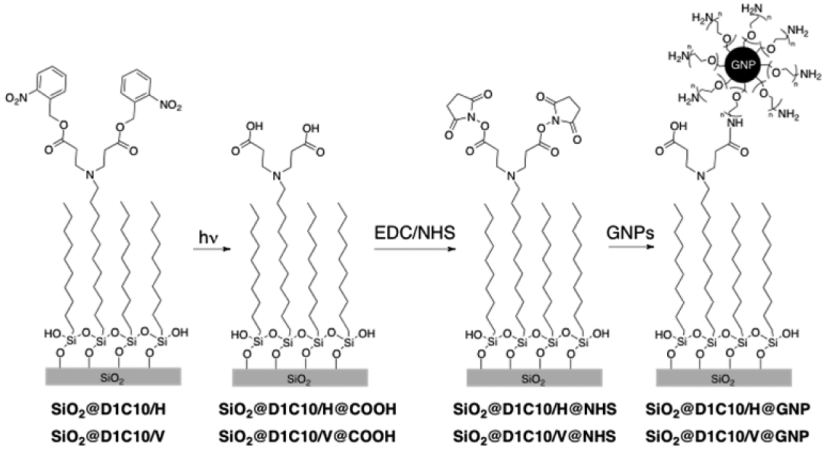

Thereafter, by modifying solvent (toluene) of the silanization reaction, a new surface **SiO_2@D1C10/V** with nanometer size domains was isolated. Contact angle value of the surface was found to be 97° ± 1 showing the hydrophobic character of the surface. PM-IRRAS spectrum of **SiO_2@D1C10/V** (Figure 1a) showed all the characteristic bands of the two organosilanes precursors as already observed for the homogeneous surface **SiO_2@D1C10/H** described above. However, we noticed that the intensities of bands are quite different for **SiO_2@D1C10/H** and **SiO_2@D1C10/V**. For **SiO_2@D1C10/H**, the νC═O (1740 cm^{-1}), $\nu_a NO_2$ (1531 cm^{-1}) and $\nu_s NO_2$ (1345 cm^{-1}) bands relative to **D1** were more intense than for the **SiO_2@D1C10/V** surface, meaning that the quantity of precursor **D1** was slightly higher for the **SiO_2@D1C10/H** surface. On the other hand, the νCH_3 (2961 cm^{-1}), $\nu_a CH_2$ (2928 cm^{-1}), and $\nu_s CH_2$ (2856 cm^{-1}) bands are slightly less intense in the case of **SiO_2@D1C10/H**. These observations are coherent with contact angles measurements in favor of a more hydrophilic surface, according to a better incorporation of **D1** precursor in the case of **SiO_2@D1C10/H**. AFM images recorded on the **SiO_2@D1C10/V** surface revealed nanometer-sized volcanolike patterns (4−6 nm of height and 100 nm of width, and around 3 volcanos/μm^2) according to AFM analysis (height and phase images) (Figure 2c−f). AFM phase images confirmed the organic chemical nature on the whole surface namely for both nanovolcanos and matrix areas (Figure 2d). Indeed, we believe that the lower solubility of **D1** in toluene than in the solvent mixture $CHCl_3$/ C_6H_{12} (25/75) is responsible for the difference of grafting kinetics between the two organosilanes (hydrosilylated **D1** and decyltrichlorosilane). The result is probably due to the phase segregation between the two organosilanes and the nanodomain structures shaped as nanovolcanos as observed on the grafted surface. We believe that the dendritic structure of the coupling agent helps to promote the phase segregation of the surface together with permitting an efficient surface functionalization. It is noteworthy that nanodesigned surfaces produced by a bottom-up approach are generally created in two steps starting from the formation of SAM or polymer monolayers followed by a shaping by lithography techniques.

Immobilization of Gold Nanoparticles Coated with Amino-PEG, on Chemically Modified Surfaces. We investigated the covalent immobilization of 20 nm gold nanoparticles (GNPs) coated with amino-polyethylene glycol, on both surfaces **SiO_2@D1C10/H** and **SiO_2@D1C10/V**, in order to resolve the chemical nature of each part of the surfaces. Namely, we used these nanoparticles coated with PEG-NH_2 as a nanoscale marker and to imitate a covalent grafting of biomolecules in the frame of biotechnology applications. The advantages of these particles, are (i) their easy detection by AFM on the surface and (ii) the PEG part of the particles to overcome their physical adsorption on surfaces.[55,56] Indeed, we wish to exclusively immobilize these particles through a covalent bonding strategy and to differentiate at the nanoscale from the functional **D1** organosilane capable to covalently react with the amino groups of GNP and the inert decylorganosilane.[57] The immobilization of GNPs was realized in three steps (Scheme 1).

Thus, the photocleavable nitrobenzyl groups[58] of **SiO_2@D1C10/H** and **SiO_2@D1C10/V** surfaces were UV-irradiated for 30 min to obtain the free carboxylic functional surfaces **SiO_2@D1C10/H@COOH** and **SiO_2@D1C10/V@COOH**. Then, these surfaces were activated by EDC/NHS to afford **SiO_2@D1C10/H@NHS** and **SiO_2@D1C10/V@NHS**. Finally, GNPs were immobilized on freshly activated surfaces, yielding **SiO_2@D1C10/H@GNP** and **SiO_2@D1C10/V@GNP** surfaces. Each step of the chemical modification was characterized by PM-IRRAS.[59] Spectra for the chemical modification of **SiO_2@D1C10/H** and **SiO_2@D1C10/V** are presented in (Figure 1b,c,d) and (Figure S1a,b,c in Supporting Information), respectively. Thus, the photocleavage of the nitrobenzyl groups was characterized by the complete disappearance of the two bands associated with the NO_2 vibrations (ν_a NO_2: 1531 cm^{-1} and $\nu_s NO_2$: 1345 cm^{-1}) and the appearance at 1721 $cm^{-1}$of a new band assigned to the stretching mode of the carbonyl of the carboxylic acid group. Then, the activation of the carboxylic acid group by EDC/NHS was observed by the appearance of three new bands at 1816, 1785, and 1741 cm^{-1} associated with NHS ring. Afterward, the GNPs covalent immobilization was characterized by the complete disappearance of the bands of the NHS ring. It is noteworthy that the methylene stretching bands observed at 2928 cm^{-1} ($\nu_a CH_2$) and 2856 cm^{-1} ($\nu_s CH_2$) as well as the methyl stretching bands at 2961 cm^{-1} are preserved for each step, revealing the perfect chemical stability of the monolayer during the chemical modification process. The **SiO_2@D1C10/H@GNP** and **SiO_2@D1C10/V@GNP** surfaces were characterized by AFM (Figure 3). Immobilized GNPs were observed in both cases by AFM (height) and KFM

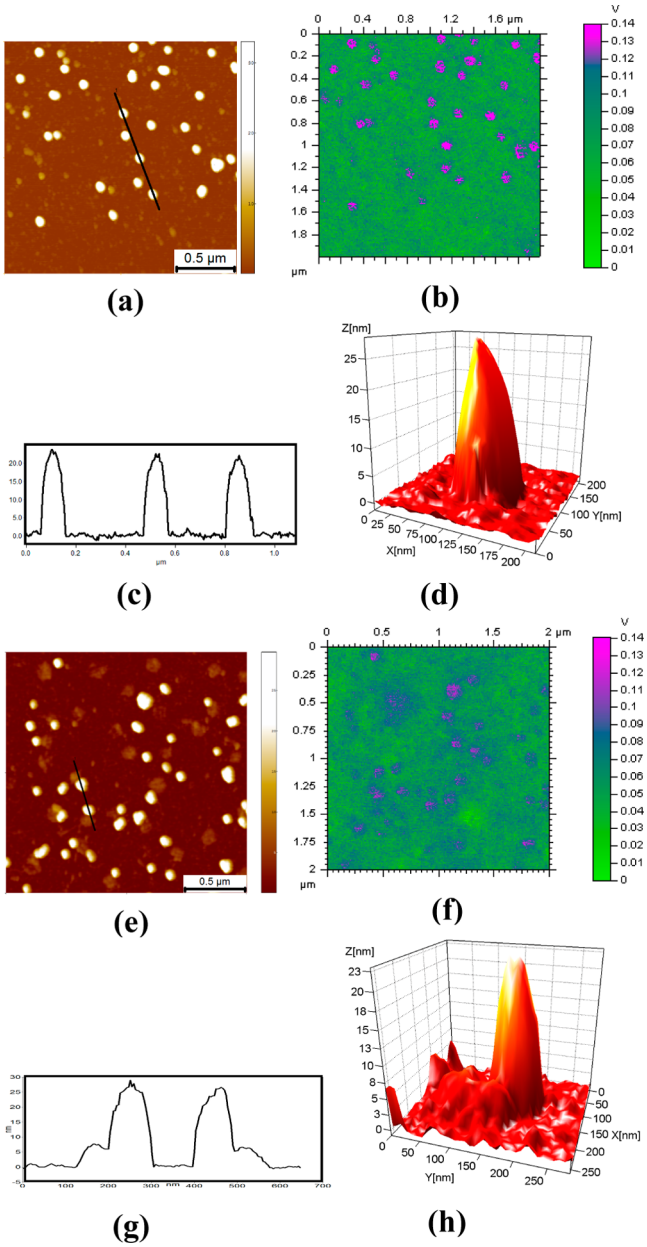

Figure 3. AFM images (2.5 μm × 2.5 μm) of **SiO_2@D1C10/H** and **SiO_2@D1C10/V** after the covalent immobilization of GNPs: (a) Height image of **SiO_2@D1C10/H**. (b) KFM image of **SiO_2@D1C10/H**. (c) Topography along a line of a. (d) 3D topography of one GNP of a. (e) Height image of **SiO_2@D1C10/V**. (f) KFM image of **SiO_2@D1C10/V**. (g) Topography along a line of Figure 3(**e**) showing the nanovolcano height and the GNP height. (h) 3D topography of GNP immobilized on one nanovolcano of e.

(Kelvin force microscopy); Conductor objects of 25−30 nm of height were measured (Figure 3b,f). The potential difference between the bright round spot and dark area are about 44 and 100 mV, respectively, for **SiO_2@D1C10/V@GNP** and **SiO_2@D1C10/H@GNP**. Surface **SiO_2@D1C10/H@GNP** revealed an homogeneous distribution of GNPs (Figure 3a−c). However, surface **SiO_2@D1C10/V@GNP** showed that GNPs are preferentially immobilized on the edges of the nanovolcano domains (Figure 3e−h). This result demonstrates the chemical nature of the surface and particularly the chemical nature of the heterogeneous surface. Therefore, the volcano-like nanostructures of **SiO_2@D1C10/V@GNP** appeared to be constituted only by **D1** organosilane precursor and the matrix areas by decylorganosilane.

In summary, we optimized a dense and well-packed grafting of a functional dendritic silylated coupling agent **D1**, inserted in a decylorganosilane monolayer, and we demonstrated that it was possible to control the formation of both an homogeneous surface **SiO_2@D1C10/H** and nanodomains designed surface **SiO_2@D1C10/V** depending on the solvent used in the silanization step, respectively $CHCl_3/C_6H_{12}$ (25/75) and toluene. The dendritic structure of **D1** was used to improve the functionalization of the grafted surface and afforded enough anchoring sites to immobilize covalently GNPs. Thus, it was possible to prove the chemical nature of the surfaces and particularly the volcano type nanodomain structures revealing a segregation of phases between organosilane precursors. Well, the functional nanodesign was straightforward achieved in a bottom-up approach without any specific lithography device and according to a versatile surface chemistry. We believe that this strategy will open new perspectives in the construction of new nanodomains patterns of interest for material science and its interfaces with chemistry and biology for the design of nanodevices as nanosensors. These surfaces illustrate the great promise for multifunctional surfaces chemistry in biotechnology and nanoengineering applications. Finally, we think that using this nanodesign bottom-up approach, biomolecules might be positioned within desired nanoregions with well-defined feature size and shape while retaining their native 3D structures and biological functionalities.

EXPERIMENTAL METHODS

Substrates for PM-IRRAS and AFM Analysis. The SiO_2/Au substrates suitable for PM-IRRAS measurements were supplied by Optics Balzers AG. They correspond to Goldflex mirror with SiO_2 protection layer 215 Å thick (Goldflex PRO, reference 200785). Silicon wafer were used for AFM and KFM analysis (performed in air at room temperature using Agilent 5500).

AFM probe are Arrow EFM Nanoworld with Pt/Ir coating. SiO_2/Au substrates and wafer slides were thoroughly washed with milli-Q water (18 MΩ.cm), immersed in chloroform and put in ultrasonic bath for 15 min. They were dried by nitrogen flux, exposed to UV-ozone (λ = 185−254 nm) for 30 min and immediately introduced to the silanization flask.

Silanization Process. The flask was prepared under vacuum for 1.5 h at 25 °C, and filled with argon and cooled to 5 °C. Freshly prepared hydrosilylated decane (4.68×10^{-5} mol) and hydrosilylated **D1** (1.56×10^{-5} mol) were dissolved with 5 mL of dried toluene or $CHCl_3/C_6H_{12}$ (25/75). The reaction mixture was then added in 120 mL of dried toluene or $CHCl_3/C_6H_{12}$ (25/75). At last, the solution was introduced into the silanization flask of containing the substrates (SiO_2/Au and wafer) immersed in 125 mL of dried toluene or $CHCl_3/C_6H_{12}$ (25/75) under argon. The temperature of silanization was controlled to be 5 °C, and the substrates were immersed in the solution for 45 min. Then, the substrates were removed from the silanization flask, cleaned using ultrasonic bath for 5 min successively with toluene, chloroform, and Milli-Q water and dried under vacuum for 30 min.

PM-IRRAS Experiments. PM-IRRAS spectra were recorded on a ThermoNicolet Nexus 670 FTIR spectrometer at a resolution of 4 cm^{-1}, by coadding several blocks of 1500 scans (30 min acquisition time). All spectra were collected in a dry-air atmosphere after 30 min of incubation in the chamber. Experiments were performed at an incidence angle of 75° using an external homemade goniometer reflection attachment, adding a ZnSe photoelastic modulator (PEM, Hinds Instruments, type III) after the polarizer.[60,61] PM-IRRAS

dx.doi.org/10.1021/am402071t | ACS Appl. Mater. Interfaces 2013, 5, 6843−6849

spectra were presented in terms of the IRRAS unit, using a calibration procedure.[62]

Deprotection of Acid Groups on the Surface. The substrates were irradiated at room temperature for 30 min. The irradiation conducted using a high-pressure mercury lamp (365 nm) coupled with a 280 nm cutoff filter (Pyrex plate) for preventing deterioration of the organic layer. The substrates were placed 2 cm far from the Pyrex plate and the Pyrex plate 3 cm far from the UV lamp. After the irradiation, the substrates were cleaned using ultrasonic bath with ethanol and chloroform for 10 min. Then, they were dried under nitrogen flow.

Activation of Acid Groups of the Surface. carboxylic acid functionalized substrates were immersed in a solution containing 20 mL of Milli-Q water, 1 g of *N*-(3-dimethylaminopropyl)-*N*′-ethyl-carbodiimide hydrochloride (EDC), 0.5 g of *N*-hydroxysuccinimide (NHS) and 1.2 g of 2-(*N*-morpholino)ethanesulfonic acid (MES) 0.3M, pH 6, for 3 h at room temperature. Then, the substrates were washed with Milli-Q water and cleaned using ultrasonic bath with chloroform (10 min) and dried under nitrogen flow.

GNPs Immobilization on the Surface. One milliliter of aqueous solution containing 3.4×10^{11} of GNPs (amino PEGylated gold nanoparticles 20 nm, supplied by Polysciences, Inc.) was added to 9 mL of phosphate buffer saline (PBS) solution adjusted to pH 8 using a solution of KOH (0.5 M). The substrates were immersed in latter solution for 20 h at 37 °C. Then, the substrates were collected, washed thoroughly with Milli-Q water, and cleaned in an ultrasonic bath (Milli-Q water) for 10 min. The substrates were dried under nitrogen flow and dried under vacuum for 30 min.

■ ASSOCIATED CONTENT

Ⓢ Supporting Information

Synthetic procedures for compounds **1** and **D1** and hydrosylilation of **D1** and dec-1-ene. Scheme S1, synthesis of dendritic coupling agent D1. Scheme S2, hydrosilylation and silanization of a mixture of **D1** and dec-1-ene (25/75). Figure S1, PM-IRRAS spectra for each step of chemical modification of the monolayer **SiO_2@D1C10/V**. This material is available free of charge via the Internet at http://pubs.acs.org/.

■ AUTHOR INFORMATION

Corresponding Author

*E-mail: k.heuze@ism.u-bordeaux1.fr, l.vellutini@ism.u-bordeaux1.fr.

Notes

The authors declare no competing financial interest.

■ ACKNOWLEDGMENTS

Financial support from the Université Bordeaux 1, Centre National de la Recherche Scientifique (CNRS), the Region Aquitaine (for HR fellowship), and the Ministère de l'Enseignement Supérieur et de la Recherche is gratefully acknowledged.

■ REFERENCES

(1) Prime, K. L.; Whitesides, G. M. *Science* **1991**, *252*, 1164−1167.
(2) Kim, D. C.; Kang, D. J. *Sensors* **2008**, *8*, 6605−6641.
(3) Ekblad, T.; Liedberg, B. *Curr. Opin. Colloid Interface Sci.* **2010**, *15*, 499−509.
(4) Floch, A.; Toner, M. *Annu. Rev. Biomed. Eng.* **2000**, *2*, 227−256.
(5) Langer, R. *Science* **2001**, *293*, 58−59.
(6) Ratner, B. D.; Bryant, S. J. *Annu. Rev. Biomed. Eng.* **2004**, *6*, 41−75.
(7) Früh, V.; Ijzerman, A. P.; Siegal, G. *Chem. Rev.* **2011**, *111*, 640−656.
(8) Gates, B. D.; Xu, Q.; Stewart, M.; Ryan, D.; Willson, C. G.; Withesides, G. M. *Chem. Rev.* **2005**, *105*, 1171−1196.
(9) Herzer, N.; Hoeppener, S.; Schubert, U. S. *Chem. Commun.* **2010**, *46*, 5634−5652.
(10) Tawfick, S.; De Volder, M.; Copic, D.; Park, S. J.; Oliver, C. R.; Polsen, E. S.; Roberts, M. J.; Hart, A. J. *Adv. Mater.* **2012**, *24*, 1628−1674.
(11) Zhou, X.; Boey, F.; Huo, F.; Huang, L.; Zhang, H. *Small* **2011**, *7*, 2273−2289.
(12) Krämer, S.; Fuierer, R. R.; Gorman, C. B. *Chem. Rev.* **2003**, *103*, 4367−4418.
(13) Walsh, M. A.; Hersam, M. C. *Annu. Rev. Phys. Chem.* **2009**, *60*, 193−216.
(14) Singh, S. C.; Zeng, H. *Sci. Adv. Mater.* **2012**, *4*, 368−390.
(15) Schmidt, R. C.; Healy, K. E. *J. Biomed. Mater. Res. A* **2009**, *90*, 1252−1261.
(16) Gooding, J. J.; Ciampi, S. *Chem. Soc. Rev.* **2011**, *40*, 2704−2718.
(17) Whitesides, G. M.; Grzybowski, B. *Science* **2002**, *295*, 2418−2421.
(18) Dinh, D. H.; Pascal, E.; Vellutini, L.; Bennetau, B.; Rebière, D.; Dejous, C.; Moynet, D.; Belin, C.; Pillot, J.-P. *Sens. Actuators, B* **2010**, *146*, 289−296.
(19) Calmark, A.; Hawaker, C.; Hult, A.; Malkoch, M. *Chem. Soc. Rev.* **2009**, *38*, 352−362.
(20) Stiriba, S. E.; Frey, H.; Haag, R. *Angew. Chem., Int. Ed.* **2002**, *41*, 1329−1334.
(21) Dahan, A.; Portnoy, M. *J. Polym. Sci., Part A: Polym. Chem.* **2005**, *43*, 235−262.
(22) Newkome, G. R.; Yoo, K. S.; Kabir, A.; Malik, A. *Tetrahedron Lett.* **2001**, *42*, 7537−7541.
(23) Lee, C. C.; MacKay, J. A.; Fréchet, J. M. J.; Szoka, F. C. *Nat. Biotechnol.* **2005**, *23*, 1517−1526.
(24) Paez, J. I.; Martinelli, M.; Brunetti, V.; Strumia, M. C. *Polymers* **2012**, *4*, 355−395.
(25) Satija, J.; Sai, V. V. R.; Mukherji, S. *J. Mater. Chem.* **2011**, *21*, 14367−14386.
(26) Bosman, A. W.; Janssen, H. M. E.; Meijer, W. *Chem. Rev.* **1999**, *99*, 1665−1688.
(27) Fréchet, J. M. J.; Tomalia, D. A. *Dendrimers and Other Dendritic Polymers*; Wiley & Sons: Chichester, U.K., 2001, and references cited therein.
(28) Newkome, G. R.; Moorefield, C. N.; Vögtle, F. *Dendrimers and Dendrons: Concepts, Syntheses, Perspectives*; Wiley-VCH: Weinheim, Germany, 2002, and references cited therein.
(29) Hierlemann, A.; Campbell, J. K.; Baker, L. A.; Crooks, R. M.; Ricco, A. J. *J. Am. Chem. Soc.* **1998**, *120*, 5323−5424.
(30) Felipe, M. J.; Estillore, N.; Pernites, R. B.; Nguyen, T.; Ponnapati, R.; Advincula, R. C. *Langmuir* **2011**, *27*, 9327−9336.
(31) Gruber, K.; Rohr, C.; Scherer, L. J.; Malarek, M. S.; Constable, E. C.; Hermann, B. A. A *Adv. Mater.* **2011**, *23*, 2195−2198.
(32) Xiao, Z.; Cai, C.; Mayeux, A.; Milenkovic, A. *Langmuir* **2002**, *18*, 7728−7739.
(33) Friggeri, A.; van Manen, H.-J.; Auletta, T.; Li, X. M.; Zapotoczny, S.; Schönherr, H.; Vancso, G. J.; Huskens, J.; van Veggel, F. C. J. M.; Reinhoudt, D. N. *J. Am. Chem. Soc.* **2001**, *123*, 6388−6395.
(34) Dong, B.; Huo, F.; Zhang, L.; Yang, X.; Wang, Z.; Zhang, X.; Gong, S.; Li, J. *Chem.—Eur. J.* **2003**, *9*, 2331−2336.
(35) Yang, M.; Tsang, E. M. W.; Wang, Y. A.; Pang, X.; Yu, H.-Z. *Langmuir* **2005**, *21*, 1858−1865.
(36) Luscombe, C. K.; Proemmel, S.; Huck, W. T. S.; Holmes, A. B.; Fukushima, H. *J. Org. Chem.* **2007**, *72*, 5505−5513.
(37) Wyszogrodzka, M.; Haag, R. *Biomacromolecules* **2009**, *10*, 1043−1054.
(38) Öberg, K.; Ropponen, J.; Kelly, J.; Löwenhielm, P.; Berglin, M.; Malkoch, M. *Langmuir* **2013**, *29*, 456−465.
(39) Rolandi, M.; Suez, I.; Dai, H.; Fréchet, J. M. *Nano Lett.* **2004**, *4*, 889−893.
(40) Zhang, Q.; Archer, L. A. *Langmuir* **2006**, *22*, 717−722.
(41) Benters, R.; Niemeyer, C. M.; Wöhrle, D. *ChemBioChem* **2001**, *2*, 686−694.

(42) Heuzé, K.; Rosario-Amorin, D.; Nlate, S.; Gaboyard, M.; Bouter, A.; Clérac, R. *New J. Chem.* **2008**, *32*, 383−387.
(43) Kehat, T.; Goren, K.; Portnoy, M. *New J. Chem.* **2007**, *31*, 1218−1242.
(44) Bu, J.; Li, R.; Quah, C. W.; Carpenter, K. J. *Macromolecules* **2004**, *37*, 6687−6694.
(45) Tomalia, D. A.; Hall, M.; Hedstrand, D. *Macromolecules* **1987**, *20*, 1164−1167.
(46) Lin, W.; Zhang, X.; He, Z.; Jin, Y.; Gong, L.; Mi, A. *Synth. Commun.* **2002**, *32*, 3279−3284.
(47) DMF was used as solvent in the Michael addition reaction instead of methanol, usually used, to avoid trans-esterification reaction of nitrobenzyl group.
(48) Wasserman, S. R.; Tao, Y.-T.; Whitesides, G. *Langmuir* **1989**, *5*, 1074−1087.
(49) Martin, P.; Marsaudon, S.; Thomas, L.; Desbat, B.; Aimé, J. P.; Bennetau, B. *Langmuir* **2005**, *21*, 6934−6943.
(50) Tong, Y.; Tyrode, E.; Osawa, M.; Yoshida, N.; Watanabe, T.; Nakajima, A.; Ye, S. *Langmuir* **2011**, *27*, 5420−5426.
(51) Choi, I.; Kim, Y.; Kang, S. K.; Lee, J.; Yi, J. *Langmuir* **2006**, *22*, 4885−4889.
(52) Tokuhisa, H.; Liu, J.; Omori, K.; Kanesato, M.; Hiratani, K.; Baker, L. A. *Langmuir* **2009**, *25*, 1633−1637.
(53) Fan, F.; Maldarelli, C.; Couzis, A. *Langmuir* **2003**, *19*, 3254−3265 and references therein.
(54) Stranick, S. J.; Parikh, A. N.; Tao, Y. T.; Allara, D. L.; Weiss, P. S. *J. Phys. Chem.* **1994**, *98*, 7636−7646.
(55) *Poly(ethylene glycol) Chemistry: Biotechnical and Biomedical Applications*; Harris, J. M., Eds.; Plenum Press: New York, 1992.
(56) Prime, K. L.; Whitesides, G. M. *J. Am. Chem. Soc.* **1993**, *115*, 10714−10721.
(57) A trial of GNPs immobilization on decylorganosilane grafted surface was realized in similar experimental conditions. As a result, no GNP was observed on the surface by AFM analysis, confirming the absence of nonspecific immobilization of the GNP on our surfaces.
(58) Zhao, H.; Sterner, E. S.; Coughlin, E. B.; Theato, P. *Macromolecules* **2012**, *45*, 1723−1736.
(59) Ramin, M. A.; Le Bourdon, G.; Heuzé, K.; Degueil, M.; Belin, C.; Buffeteau, T.; Bennetau, B.; Vellutini, L. *Langmuir* **2012**, *28*, 17672−17680.
(60) Buffeteau, T.; Desbat, B.; Turlet, J.-M. *Appl. Spectrosc.* **1991**, *45*, 380−389.
(61) Ramin, M. A.; Le Bourdon, G.; Daugey, N.; Bennetau, B.; Vellutini, L.; Buffeteau, T. *Langmuir* **2011**, *27*, 6076−6084.
(62) Buffeteau, T.; Desbat, B.; Blaudez, D.; Turlet, J.-M. *Appl. Spectrosc.* **2000**, *54*, 1646−1650.